Accepted Manuscript

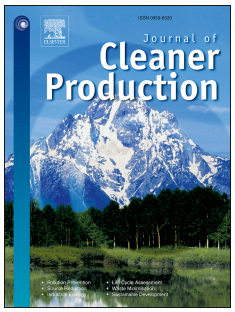

Assessment of *Miscanthus* × *giganteus* derived biochar as copper and zinc adsorbent: Study of the effect of pyrolysis temperature, pH and hydrogen peroxide modification

Alessio Cibati, Bente Foereid, Ajay Bissessur, Simona Hapca

PII: S0959-6526(17)31285-4

DOI: 10.1016/j.jclepro.2017.06.114

Reference: JCLP 9864

To appear in: *Journal of Cleaner Production*

Received Date: 13 December 2016

Revised Date: 13 June 2017

Accepted Date: 13 June 2017

Please cite this article as: Cibati A, Foereid B, Bissessur A, Hapca S, Assessment of *Miscanthus* × *giganteus* derived biochar as copper and zinc adsorbent: Study of the effect of pyrolysis temperature, pH and hydrogen peroxide modification, *Journal of Cleaner Production* (2017), doi: 10.1016/j.jclepro.2017.06.114.

Assessment of *Miscanthus x giganteus* derived biochar as copper and zinc adsorbent: study of the effect of pyrolysis temperature, pH and hydrogen peroxide modification

Alessio Cibati[a,d*], Bente Foereid[b,d], Ajay Bissessur[a], Simona Hapca[d]

[a]School of Engineering, University of KwaZulu-Natal, Howard College Campus, Durban, South Africa

[b]NIBIO, Norwegian Institute of Bioeconomy Research, Norway

[a]School of Chemistry and Physics, University of KwaZulu-Natal, Howard College Campus, Durban, South Africa

[d]SIMBIOS Centre, Abertay University of Dundee, Bell Street, Dundee (Scotland, UK)

*Corresponding author: e-mail: cibale1983@gmail.com

Abstract

In this work, experimental and modelling investigations were conducted on biochars pyrolyzed at 350°C and 600°C, to determine the effect of pyrolysis temperature, hydrogen peroxide activation and pH on copper and zinc removal, in comparison with commercially available activated carbons. Characterization of biochars was performed by BET surface area, elemental analysis and FTIR spectroscopy. Experiments results demonstrated that biochar pyrolyzed at 600°C adsorbed both copper and zinc more efficiently than biochar pyrolyzed at 350°C. Chemical activation by H_2O_2 increased the removal capacity of biochar pyrolyzed at 350°C. All investigated biochars showed a stronger affinity for copper retention, with a maximum adsorption capacity of 15.7 mg/g while zinc was 10.4 mg/g. The best adsorption performances were obtained at pH 5 and 6. Langmuir adsorption isotherm described copper adsorption process satisfactorily, while zinc adsorption was better described by Freundlich isotherm.

Keywords: Biochar; metal adsorption; isotherms; adsorbent; copper; zinc

1. Introduction

Environmental contamination by metals has become a serious problem due to their indefinite persistence in the environment which lead to water, air and soil contamination and health risks Metals can be released into the environment from several industrial processes such as mining, metal processing, automobile manufacturing, refining of ores and combustion of fossil fuels (Tchounwou et al., 2012; Margui et al., 2004). Copper and zinc are widely used for many purposes like electrical appliances, electronics, automotive, paint and battery, as well as compounds in fungicides, algicides, insecticides, fertilisers and pesticides. Given their toxic effect, their discharge into the environment can pose risk for human health. The limits in drinking water are 1 mg/L and 5 mg/L for copper and zinc, (Secondary Maximum Contaminant Level) (EPA, 2016).

In the past years, methods such as Fenton- chemical precipitation (Fu et al., 2012), ion-exchange (Dabrowski et al., 2004), , membrane filtration (Malamis et al., 2011), electro-coagulation (Akbal and Camci, 2011) and adsorption (Boudrahem et al., 2011; F Turan et al., 2011) among the others, have been optimized to regenerate waters and industrial wastewaters contaminated by heavy metals.

Boudrahem et al. (2011), studied modified activated carbons derived from coffee residue through a chemical activation using zinc chloride and phosphoric acid, which led to a modification of the pore structure and enhanced the adsorption capacity of the adsorbent. Similarly, Trevino-Cordero et al. (2013), proved the suitability of fruits plant derived activated carbons for the removal of contaminants in water and showed the positive effects of impregnation with calcium salts on the surface of the activated carbons. Currently, adsorption has been proved as one of the most promising techniques and activated carbon (AC) is currently one of the most used adsorbents in such treatments. However, the necessity to find more cost-effective treatments have led researchers to explore the feasibility of low-cost

materials as metals adsorbent. Materials like zero valent iron, agricultural waste such as nut shell, fruit bagasse, rice and coconut husk, egg shells, seafood waste and chitosan have been investigated as material for the removal of metals and other pollutants from water (Lim and Aris, 2013). Other researchers have investigated the production and use of biochar from feedstocks such as plant residues (Chen et al., 2011; Yao et al., 2011), animal manures (Cao and Harris, 2010), sewage sludge (Wang et al., 2011) and swine manure (Meng et al., 2014)

Biochar is a carbon rich material produced by combustion under reduced oxygen supply (pyrolysis) of organic (plant, wood, agricultural waste, sludge, poultry litter) materials. *Miscanthus x giganteus* is a plant grown in Europe and widely studied as energy crops (Lewandowski et al., 2000; Brosse et al., 2012), crop for co-firing with coal to produce power and reduce CO_2 emission (Heaton et al., 2004; Clifton-Brown et al., 2007), feedstock for second generation biofuels (; Melligan et al., 2012) and as soil amendment (; Kwapinski et al., 2010 Houben et al., 2014). Despite *Miscanthus x giganteus* derived biochar has been proved as a suitable soil amendment, and has shown good physical/chemical properties for metals uptake (Mimmo et al., 2014), no studies have been conducted so far to test the capacities of *Miscanthus x giganteus* derived biochar to adsorb metals from aqueous solutions. Mimmo et al. (2014), pointed out the effect of pyrolysis temperature on biochar structure showing physic/chemical changes of surface and porous structure, indicating 360°C as threshold above which aromatic structures increase and O/C and H/C ratios decrease.

In this framework, this study investigated the capacities of a biochar derived from *Miscanthus x giganteus* plant as copper and zinc adsorbent. Being adsorption influenced by many factors including pH, pyrolysis temperature, and presence of oxygen-containing functional groups on adsorbent's surface, a comprehensive investigation on *Miscanthus x giganteus* derived biochar under different operating conditions was conducted along with modelling studies through equilibrium isotherm equations. Moreover, two types of activated carbons (AC

Fluval and AC Norit) were tested for comparison. *Miscanthus x giganteus* raw biomass, due to its low performance was included in the study as a control.

2. Materials and Methods

2.1 *Miscanthus x giganteus* biochar

Feedstock for the biochar used in this study *Miscanthus x giganteus*, a perennial warm-season (C4) grass, was sourced from Adare, Limerick, Ireland. Biochar was produced by pyrolysis in a furnace at 250 atm at two different temperature, 350°C and 600°C (BC350 and BC600, respectively) for 10 min using nitrogen gas to prevent complete combustion; then it was cooled for 10 min in a tube under a nitrogen rich atmosphere.

2.2 Activated carbon

Two types of commercially available activated carbon (AC norit and AC fluval) were used in this study. AC norit, a granular activated carbon produced by steam activation of coal, has an average diameter of 1 mm, is suitable for potable water processing and industrial process liquids. Fluval carbon, a pure activated carbon is used in both fresh and salt water treatments. The inner matrix structure provides a large porous area that permanently traps organic and inorganic wastes and removes many other impurities from the water.

2.3 Chemical and physical characterisation of biochars

The specific surface areas (SA) were measured with N_2 (g) adsorption at 77 K determined by a Tristar II3020 surface area analyzer (Micromeritics Instrument Co., USA). Specific surface areas (SBET) were taken from adsorption isotherms using the Brunauer, Emmett and Teller (BET) equation (Brunauer et al., 1938). Elemental analysis of carbon (C), hydrogen (H), oxygen (O) and nitrogen (N) was conducted by ThermoScientific Flash 2000 organic

elemental analyser. FT-IR analysis was conducted using a Perkin Elmer Spectrum RX1 FT-IR spectrometer to establish the nature of the biochar and the changes to the structure as a consequence of both pyrolysis and chemical activation.

2.4 Adsorption batch experiments

Batch experiments were performed to investigate the adsorption capacity of biochar and activated carbon on copper and zinc metal ions from aqueous solutions. In each experiment, an aliquot mass of 1 g of adsorbent was mixed with 50 mL of Cu^{2+} (aq) and Zn^{2+} (aq) solutions at different initial concentrations (mg/L): 63.5; 158.5; 317.7; 635.4; 1,270.8 for copper solutions, and 65.3; 163.4; 327; 653.8; 1,307.6 (mg/L) for zinc solutions in a 250 mL Erlenmeyer flask. The Cu^{2+} (aq) and Zn^{2+} (aq) ions were introduced in the synthetic solutions as copper sulfate ($CuSO_4 \cdot 5H_2O$) and zinc sulfate ($ZnSO_4 \cdot 7H_2O$). All chemicals used were of analytical grade supplied by Sigma Aldrich. Solutions were prepared with ultrapure water produced by Milli-Q gradient unit (Millipore). Initial tests showed that the amount removed had stabilised after 1 hour (h), for this reason each experiment was carried out for 1 h. The mixture was agitated at 120 rpm on a shaker at room temperature and samples were taken at intervals of 15 min. The samples then were immediately filtered with 0.45 µm Whatman filter and the filtrates were analysed for residual metals concentrations in solution by Atomic Absorption Spectroscopy (AAnalysist 200 Perkin Elmer Inc, Shelton CT, USA). All batch experiments conducted in this work were conducted in a duplicate way.

2.4.1 Operative conditions

Different sets of experiments were carried on in order to optimize the adsorption process by investigating the effect of pyrolysis temperature, pH value, modification by H_2O_2.

2.4.1.1 Pyrolysis temperature

The effect of the pyrolysis temperature on the adsorption capacity of biochar was investigated by comparing samples BC350, BC600 and raw *Mischantus x giganteus*. Batch tests were conducted as described above.

2.4.1.2 Chemical activation by H_2O_2

Biochars, BC350 and BC600, were both pyrolyzed at 350 and 600°C and chemically activated using H_2O_2 as follows: A 3.0 g mass aliquot of BC was added to 40 ml of H_2O_2(aq) solution (10 % w/v) for 2hrs with continuous agitation at room temperature. After rinsing with de-ionized water and drying at 80°C, the resulting activated BC350 and BC600 (BC350 ACT and BC600 ACT) were stored in a sealed plastic container in a cold room at 4°C for later experiments. The adsorption capacity of BC350 ACT and BC600 ACT was investigated in batch experiments and compared to BC350, BC600, AC norit and AC fluval.

2.4.1.3 pH value

The effect of pH was studied by settling experiments at pH 4, 5 and 6. The pH during the experiment was constantly monitored and kept constant by adding drops of NaOH and HCl (0.1 M). All batch experiments were conducted as described above in the section 2.4.

2.5 Model formulation and statistical analysis

Pseudo-first-order (Eq. 1) and pseudo-second-order (Eq. 2) models were used to simulate the sorption kinetics data (Lagergren, 1898; Ho and McKay, 1999):

$$\log(q_e - q_t) = \log q_e - \frac{K_1 t}{2.303} \quad (1)$$

$$\frac{\mathrm{t}}{\mathrm{q_t}} = \frac{1}{K_2 Q_e^2} + \frac{\mathrm{t}}{\mathrm{q_e}} \quad (2)$$

where q_t and q_e (mg/g) are adsorbed copper and zinc amount at time t (h) and equilibrium, K_1 (1/h) and K_2 (g/(mg h)) are the rate constant for the pseudo-first-order and pseudo-second-order adsorption kinetics, respectively. The linear plots of value $\log(q_e - q_t)$ against

time, can give the pseudo-first-order adsorption rate constant K_1 from the slope and q_e can be calculated from the intercept. By plotting t/q_t against time t, the pseudo-second-order adsorption rate constant K_2 and q_e were determined from the intercept and slope of the plot. The corresponding values of K_1, q_e and R^2 are presented in Table 3 at tested metals concentrations. Adsorption models based on Langmuir and Freundlich equations were fitted to the data. The Langmuir model assumes monolayer adsorption onto a homogeneous surface with no interactions between the adsorbed molecules. The Freundlich model is an empirical equation commonly used for heterogeneous surfaces in the low to intermediate concentration range adsorption system (Gerente et al., 2007;). The concentration of Cu^{2+} (aq) and Zn^{2+} (aq) sorbed onto BC was calculated according to the following equation ():

$$Q_e = \frac{V(C_0 - Ce)}{g} \quad (3)$$

where Qe (mg/g) is the amount of Cu^{2+}(aq) or Zn^{2+}(aq) adsorbed at equilibrium. C_0 and Ce (mg/L) are the initial and equilibrium Cu^{2+}(aq) or Zn^{2+}(aq) concentration in solution. g (gram) is the mass of BC. The experimental data were fitted by Langmuir and Freundlich isotherms according to the following equations:

$$\text{Langmuir: } Q_e = \frac{KQmaxCe}{1+KC_e} \quad (4)$$

Where Q_e is the amount of metal adsorbed per unit weight of adsorbent (mg/g), Ce is the equilibrium concentration of solute bulk solution (mg/L), Q_{max} is the maximum monolayer adsorption capacity (mg/g) and k is the constant related to free energy.

$$\text{Freundlich } Q_e = K_f C_e^{\frac{1}{n}} \quad (5)$$

Where Q_e is the amount of solute adsorbed per unit weight of adsorbent (mg/g), Ce is the equilibrium concentration of solute in solution (mg/L), K_f is the relative adsorption capacity constant of the adsorbent (mg/g) and n is the Freundlich linearity constant and it is indicative of bond energies between metal ion and the adsorbent. The Freundlich constants can be

obtained from the plot of Ln Q_e against Ln C_e. Statistical analysis was performed in R Statistical Package v.2.12,® and comparison of the two models' performance was conducted based on the AIC model selection criterion (Fox, 2008) as provided in R. It was determined if the coefficients in the equation were different from 0 and treatments were compared pairwise to determine if the coefficients for the equations for different treatments were different from each other. Separate pairwise comparisons were carried out between types of biochar or activated carbon within each pH level, and between pH levels within each biochar/activated carbon. Furthermore, a study of the adsorption selectivity of copper and zinc by the biochars was conducted by analyzing the distribution coefficient (K_d cm^3/g). Kd is an indicator used for the selectivity of the adsorbent to the particular ion in the presence of other ions (Lin et al., 2001):

$$Kd = \frac{C0-Cf}{Cf} * \frac{V}{g} \quad (6)$$

where C_0 and C_f (mg/cm^3) are the initial and equilibrium concentrations of a metal species, respectively. V (cm^3) is the volume of the solution, and g (gram) is the amount of adsorbent. A selectivity coefficient (α), (dimensionless), for the binding of a specific metal ion in the presence of others is given by (Kang et al., 2004):

$$\alpha = \frac{Kd(T)}{Kd(I)} \quad (7)$$

where K_d(T) is the K_d value of the targeted metal (Cu^{2+}(aq) ions in this case), and K_d(*I*) is the K_d value of zinc. The greater the value of α, the better the selectivity toward copper over zinc.

3. Results and discussion

3.1 Biochar characterization

The physico-chemical characteristics of biochars (both activated and non-activated) used in this study are shown in Table 1. BET analysis showed that the pyrolysis temperature do not

remarkably affect the surface area, while the pore size of BC600 was about twice the size of BC350. Chemical activation of biochar pyrolyzed at lower temperature (BC350 ACT) showed a significant increase in BET surface area from 0.71 to 6.50 m^2/g relative to inactivated biochar (BC350) (Table 1). However, a small increase from 0.72 to 0.95 m^2/g was observed for chemical activation of biochar (BC600 ACT) relative to the inactivated biochar (BC600) (Table 1). The negligible increase in surface area for biochar pyrolyzed at higher temperature could be due to the increase of volatile fractions which reduce the pores availability (Wang et al., 2016). Chemical activation also increased the micropore volume for both biochars, while had a negligible effect on the pore size for biochar pyrolyzed at lower temperature and detrimental effect on biochar pyrolyzed at 600°C. The pH of the biochar samples treated with H_2O_2 was lower respect to the natural counterpart, which can be attributed to the presence of carboxyl surface functional groups, as observed by other authors (Huff and Lee, 2016; Xue et al., 2012). In addition, Huff and Lee (2016) also showed a higher cation exchange capacity (CEC) after H_2O_2 activation due to the addition of acidic oxygen functional groups on the surface of the biochar.

Table 1. Physiochemical properties of biochars.

Adsorbent	pH -	BET surface area (m^2/g)	t-PLOT Micropore volume (cm^3/g)	Pore size (nm)
BC350	8.30	0.71	0.000701	5.78
BC600	5.97	0.72	0.000334	11.48
BC350 ACT	5.82	6.50	0.0024	6.43
BC600 ACT	5.40	0.95	0.0014	5.40

Elemental analyses as well as O/C and H/C ratios are helpful indicators to provide biochars' characterization. Results (Table 2) indicate that an increase of pyrolysis temperature reflected a higher loss of oxygen and hydrogen content, while the carbon content increased. As a consequence of dehydration and decarboxylation reactions which occur at higher temperature, BC600 showed a decreased O/C and H/C ratios, leading to a more stable

aromatic-like structure. On the other hand, chemical activation had a noticeable effect on the oxygen content of BC350, resulting in the highest O/C ratio, highest oxygen percentage and lowest carbon percentage for the substrate, due to an increase of the oxygen-containing groups and negative charges(Table 2), as also observed by others (Wang et al., 2016).

Table 2. Elemental analysis of biochars.

Adsorbent	N (%)	C (%)	H (%)	O (%)	O/C	H/C
BC350	0.77	64.48	3.85	14.82	0.22	0.05
BC600	0.30	73.99	2.23	6.91	0.09	0.03
BC350 ACT	1.07	62.4	3.74	20.19	0.32	0.05
BC600 ACT	0.38	77.79	2.40	6.01	0.07	0.03

The Fourier transform infrared spectroscopy (Figure 1) was used as an effective qualitative tool in investigating functional group changes during the pyrolysis of biochars. For pyrolyzed biochar the important stretching vibrations are the O-H at 3400 cm^{-1}, the aliphatic C-H stretch between 3000-2860 cm^{-1}, the aromatic C-H stretch at 3060 cm^{-1}, the carboxyl (C=O) stretch at 1700 cm^{-1}, aromatic ring stretching modes at 1590 and 1515 cm^{-1}, the C-O-(C) stretch at 1275 cm^{-1} and the C-O-(H) stretch at approx. 1050 cm^{-1}. According to Sun and Tomkinson, (2001) and Bouwman and Freriks (1980), the spectral band at 1600 cm^{-1} can be due to the aromatic skeletal mode. BC350 and BC350 ACT spectra are similar to each other but more intense than the BC600 and BC600 ACT spectra. Both BC350 and BC 350ACT are dominated by stretching frequencies of the OH at between 3400 cm^{-1} to 3600 cm^{-1}, the C-H stretching between 3000 cm^{-1} and 2800 cm^{-1}, aromatic skeletal mode at approx. 1600 cm^{-1} and the C-O-(H) stretch at approx. 1050 cm^{-1}.

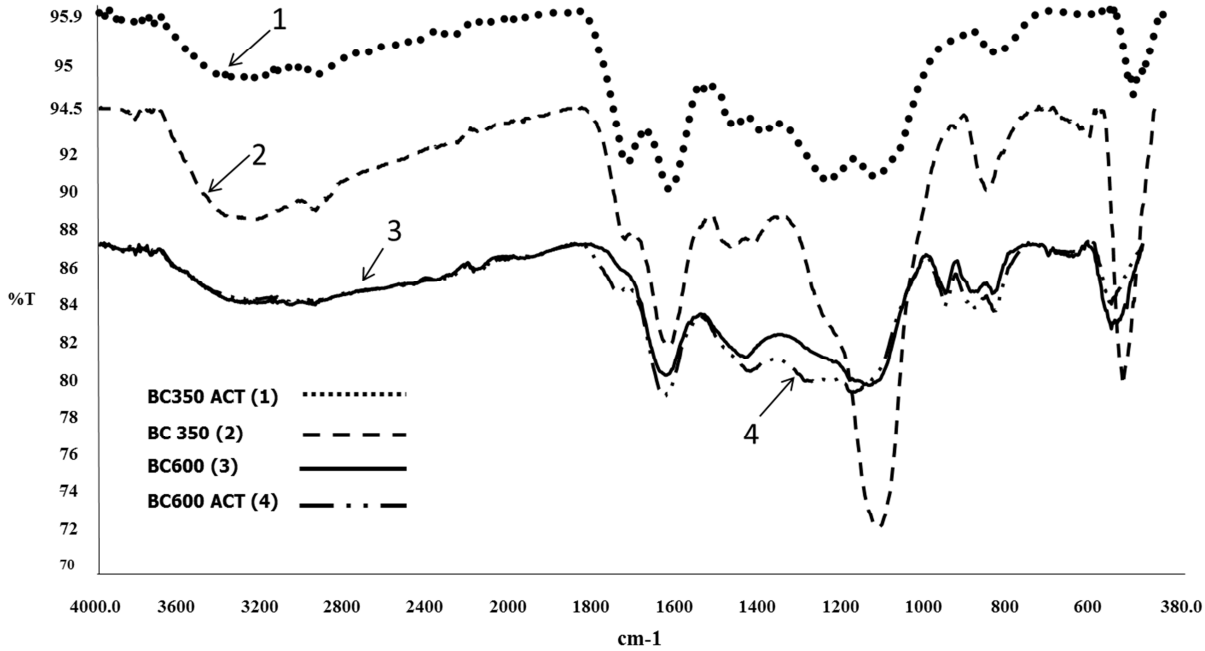

Figure 1. FT-IR analysis of all biochars investigated.

The BC350 sample showed much larger absorption energies than the BC350ACT samples due to O-H bond stretching at around 3300cm^{-1}, C-O $^{+}$=C or C=O stretches at 1600 cm^{-1} and C-O stretch at around 1100 cm^{-1} than the BC350ACT samples.

Moreover, a decreased intensity related to an increased transmittance was observed for bands associated with aromatic groups (1580-1600 and 3050-3000 cm^{-1}). These results are in accordance with previous studies (Al-Wabel et al., 2013; Yuan et al., 2011; Novak et al., 2009), which have shown that the presence of functional groups are associated with biochar pyrolyzed at lower temperature (300-500°C) and are absent or negligible at higher temperature (500-700°C). These data are in accordance with those of the atomic ratios (Table 2) which indicated a decrease of oxygen group and an increase of C-structure, leading to a decrease of biochar's polarity and to an increase of the aromatic structure at higher temperature. Similarly, Huff and Lee (2016), observed changes between treated and untreated samples occurred at 1585 cm^{-1} (C=C stretching), indicating that the H_2O_2 treatment caused an alteration of the aromatic carbon content. Conversely, the H_2O_2 treatment caused an increase

of the peaks (1315 and 1700 cm^{-1}) correlated with the carboxylic functionality (Fig.1) as also observed by Huff and Lee (2016).

In the finger printing region (1100-500 cm^{-1}), higher temperature induced an aromatic C-H deformation (850-800 cm^{-1}). Similar vibrations in the fingerprint region of *Mischantus x giganteus* biochar pyrolyzed at different temperature were also observed by Mimmo et al. (2014). In this region, also the H_2O_2 treatment led to an increase in C-H stretching probably due to conversion from aromatic C=C ring structure (Wang and Griffiths, 1985; Huff and Lee, 2016). Biochar pyrolyzed at 600°C showed less intense infrared peaks due to an increase in the carbon activity and with progression of the pyrolysis at 600°C there is evident disappearance of O-H and C-H stretches mainly due to dehydration. It is possible at this stage that the C-H peaks move from aliphatic to becoming aromatic C-H peaks and then disappear as suggested by Cheng, et al. (2008). The BC 600 and BC 600 ACT spectra are similar and are dominated by the stretching aromatic skeletal mode at 1600 cm^{-1} and the C-O-(H) stretch at 1050 cm^{-1}.

3.2 Batch experiments results

3.2.1 Adsorption kinetics

The effect of the contact time on the adsorption of copper and zinc (at pH 6) was studied (Fig. 2 and 3, respectively). Pseudo-first-order and pseudo-second-order models where applied to describe the copper and zinc kinetics removal and the obtained kinetics parameters were reported in Table 3.

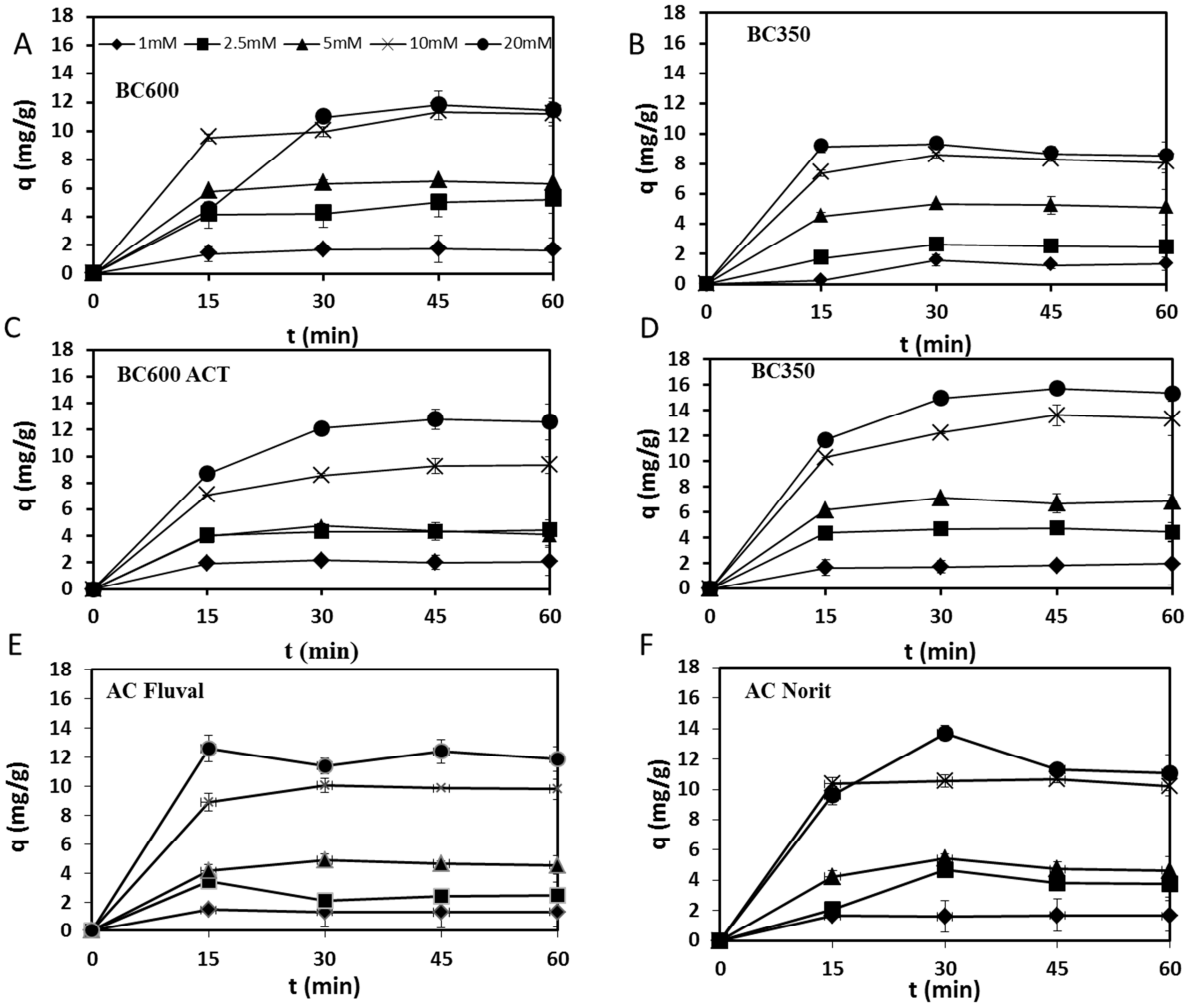

Figure 2. Effect of contact time on copper adsorption capacities at pH 6 for BC600 (A), BC350 (B), BC600ACT (C), BC350ACT (D), AC Fluval (E) and AC Norit (F).

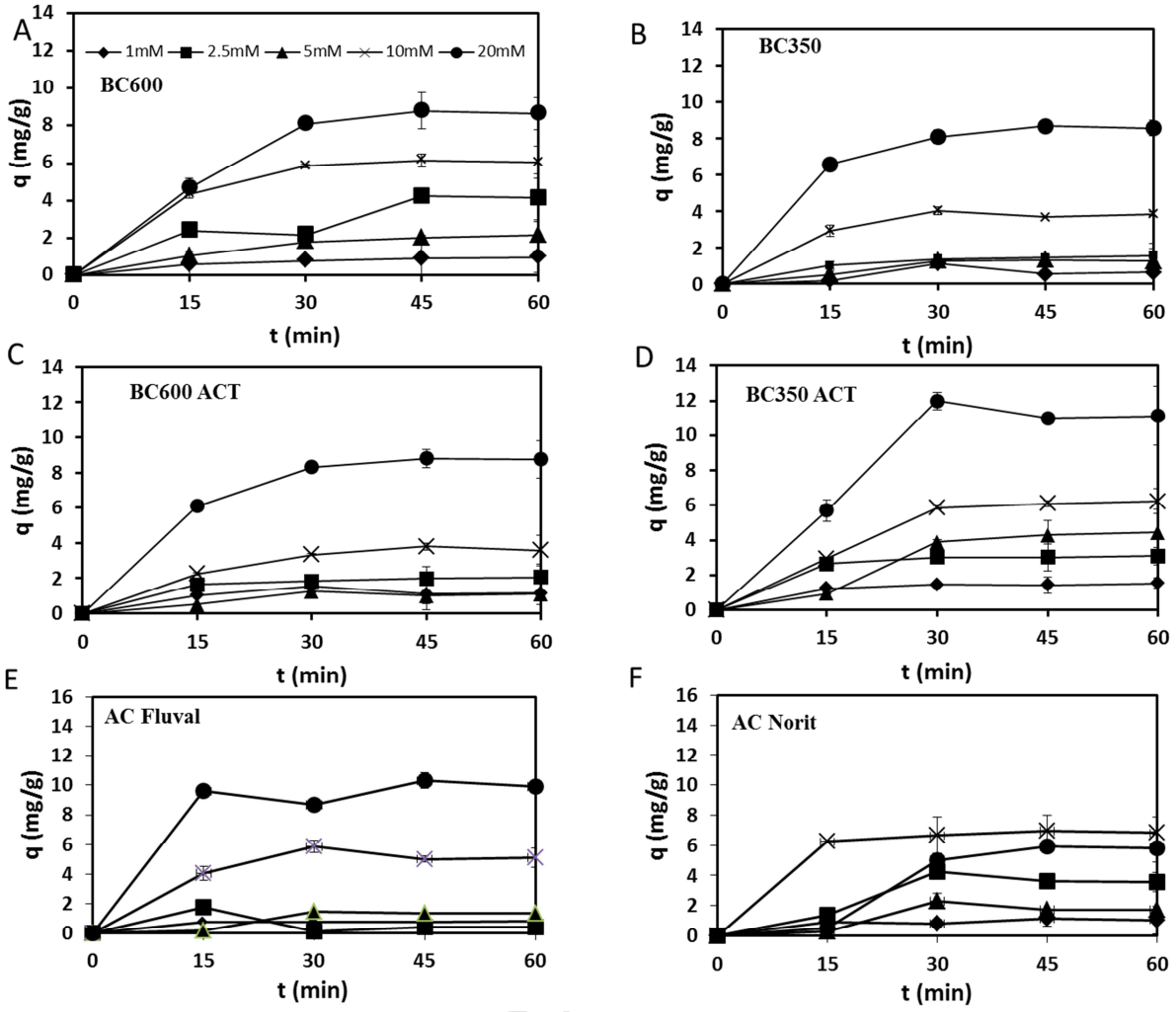

Figure 3. Effect of contact time on zinc adsorption capacities at pH 6 for BC600 (A), BC350 (B), BC600ACT (C), BC350ACT (D), AC Fluval (E) and AC Norit (F).

Metals adsorption was fast, with more than 60-70 % of adsorption occurring within 15 min, while after 30 min more than 90% of the total adsorption occurred. Similar results were also observed from Mohan et al. (2007), with 40–70% of the total metal adsorption occurred within the 60 min. Similarly to others (Moreira and Alleoni, 2010), the amount of adsorbed metal increased as the initial concentration increased (Fig. 2 and 3), as well as the competition among the metals for the adsorption sites. As matter of result, copper was preferentially adsorbed than zinc onto the four different substrates. The higher affinity of copper over zinc and other metals was also observed for other organic matrices by Fontes and Gomes (2003). Fontes et al. (2000), pointed out that zinc is more influenced by electrostatic

interactions with the active sites of the surface, whereas copper is more affected by covalent binding, and this is given by the higher ionic potential (ratio between the charge and radius of an ion) of copper (5.48) respect to zinc (5.33), confirming a greater ability of copper to bind through electrostatic interactions. Despite related works (Xue et al., 2012), showed a faster adsorption after the modification by hydrogen peroxide of peanut biochar, in this case, the modification of biochar by hydrogen peroxide did not increase the adsorption rate, but an increased amount of metal removal was observed for modified biochars pyrolyzed at lower temperature (Fig. 2D, 3D and Fig. 5). As showed in Table 2, the enhanced adsorption capacity of oxidized biochar produced at lower temperature is explained by the increase of O/C ratios, a greater drop of pH and by an increase of negative charges on the biochar surface who lead to a higher attraction of positive charged metal cations . Experimental results were fitted by pseudo-first-order and pseudo-second-order kinetic models to better describe the heavy metal adsorption mechanism. The values K_1 and K_2, calculated q_e values and the correlation coefficients R^2 are reported in Table 3.

Table 3. Parameters of pseudo-first-order and pseudo-second-order kinetics models for copper and zinc adsorption onto BC600 ACT, BC350 ACT, BC600 and BC350.

Adsorbent	Metal	pH	Initial Conc. Cu	Pseudo-first-order model			Pseudo-second-order model			Metal	pH	Initial Conc. Zn	Pseudo-first-order model			Pseudo-second-order model		
			mg/L	K_1	Qe	R^2	K_2	Qe	R^2			mg/L	K_1	Qe	R^2	K_2	Qe	R^2
BC600 ACT	**Cu**	**6**	**63.5**	0.018	0.66	0.34	2.56	2.08	0.99	**Zn**	**6**	**65.3**	0.0073	0.79	0.15	0.95	1.15	0.97
			158.5	0.0028	1.11	0.88	0.28	4.55	0.99			**163.4**	0.021	1.51	0.94	0.22	2.08	0.99
			317.7	0.0076	3.31	0.22	0.31	4.35	0.99			**327**	0.012	0.47	0.42	0.11	1.22	0.87
			635.4	0.012	3.80	0.98	0.04	10.00	0.99			**653.8**	0.022	3.02	0.75	0.06	4.00	0.96
			1,270.8	0.0039	1.11	0.82	0.02	14.29	0.98			**1,307.6**	0.03	7.24	0.90	0.03	10.00	0.98
	Cu	**5**	**63.5**	0.009	0.51	0.25	1.25	1.22	0.99	**Zn**	**5**	**65.3**	0.001	0.15	0.003	1.56	0.31	0.95
			158.5	0.022	1.29	0.88	0.33	2.13	0.99			**163.4**	0.019	1.08	0.95	0.13	1.14	0.94
			317.7	0.025	2.69	0.91	0.13	3.70	0.99			**327**	0.023	1.55	0.95	0.15	1.85	0.98
			635.4	0.022	4.17	0.75	0.02	4.55	0.86			**653.8**	0.034	5.25	0.89	0.06	6.67	0.99
			1,270.8	0.013	2.82	0.92	0.08	3.23	0.97			**1,307.6**	0.003	4.68	0.12	0.03	5.56	0.92
	Cu	**4**	**63.5**	0.005	0.28	0.49	2.81	0.08	0.89	**Zn**	**4**	**65.3**	0.006	0.19	0.85	0.67	0.13	0.80
			158.5	1.E-05	1.26	0.0001	1.01	0.09	0.98			**163.4**	0.009	0.54	0.73	2.35	0.18	0.89
			317.7	0.022	1.82	0.78	0.12	2.78	0.98			**327**	0.014	2.45	0.92	0.21	2.63	0.98
			635.4	0.0002	1.78	0.001	0.25	0.89	0.99			**653.8**	0.0012	2.09	0.002	0.03	2.94	0.76
			1,270.8	0.0321	8.32	0.98	0.009	7.69	0.85			**1,307.6**	0.004	0.86	0.03	0.05	14.29	0.99
BC350 ACT	**Cu**	**6**	**63.5**	0.018	1.32	0.88	0.28	1.96	0.99	**Zn**	**6**	**65.3**	0.017	1.06	0.84	0.35	1.56	0.99
			158.5	0.027	2.51	0.88	1.21	4.55	0.99			**163.4**	0.021	1.74	0.83	0.28	3.13	0.99
			317.7	0.0008	1.78	0.03	0.33	7.14	0.99			**327**	0.024	5.37	0.95	0.004	7.14	0.93
			635.4	0.029	10.23	0.83	0.03	14.29	0.99			**653.8**	0.033	6.92	0.97	0.02	7.14	0.90
			1,270.8	0.031	10.23	0.74	0.03	16.67	0.99			**1,307.6**	0.0048	1.20	0.03	0.01	12.5	0.92
	Cu	**5**	**63.5**	0.006	0.66	0.19	0.89	1.23	0.99	**Zn**	**5**	**65.3**	0.0018	0.13	0.01	3.88	0.81	0.98
			158.5	0.022	1.51	0.78	0.43	3.13	0.99			**163.4**	0.021	2.34	0.97	0.05	2.17	0.90
			317.7	0.024	3.39	0.94	0.10	5	0.99			**327**	0.0015	1.32	0.14	0.10	2.38	0.97
			635.4	0.023	6.46	0.96	0.05	8.3	0.99			**653.8**	0.028	5.37	0.91	0.10	8.33	0.99
			1,270.8	0.034	12.30	0.95	0.0001	33.3	0.93			**1,307.6**	0.023	0.13	0.69	0.01	11.11	0.86
	Cu	**4**	**63.5**	0.016	0.66	0.98	0.24	0.67	0.95	**Zn**	**4**	**65.3**	0.015	0.49	0.95	0.37	0.5	0.95
			158.5	0.016	0.95	0.89	2.28	1.13	0.99			**163.4**	0.012	0.87	0.93	0.05	0.77	0.90
			317.7	0.023	2.82	0.81	0.08	3.75	0.98			**327**	0.013	2.88	0.89	0.07	3.33	0.97
			635.4	0.034	5.13	0.89	0.001	11.11	0.96			**653.8**	0.022	3.98	0.99	0.03	3.85	0.90
			1,270.8	0.028	7.94	0.91	0.03	6.96	0.93			**1,307.6**	0.018	3.16	0.96	0.02	2.86	0.79
BC600	**Cu**	**6**	**63.5**	0.017	1.04	0.71	0.50	1.71	0.99	**Zn**	**6**	**65.3**	0.015	0.99	0.98	0.17	1.03	0.96
			158.5	0.028	4.79	0.95	0.06	5.31	0.98			**163.4**	0.027	5.13	0.77	0.02	4.55	0.92
			317.7	0.024	2.82	0.71	0.25	6.46	0.99			**327**	0.022	2.34	0.99	0.05	2.38	0.92
			635.4	0.03	7.94	0.81	0.04	11.44	0.99			**653.8**	0.028	4.37	0.84	0.05	6.25	0.98
			1,270.8	0.034	11.48	0.69	0.01	12.99	0.89			**1,307.6**	0.034	8.51	0.79	0.02	9.09	0.94
	Cu	**5**	**63.5**	0.018	0.59	0.84	0.47	0.81	0.98	**Zn**	**5**	**65.3**	0.009	0.47	0.51	0.12	0.5	0.90
			158.5	0.014	0.92	0.56	0.50	1.47	0.99			**163.4**	0.02	1.38	0.98	0.07	1.37	0.88
			317.7	0.01	2.40	0.64	0.48	3.23	0.99			**327**	0.001	2.88	0.57	0.05	2.86	0.93
			635.4	0.025	4.79	0.86	0.06	6.67	0.98			**653.8**	0.027	6.46	0.78	0.06	11.11	0.99
			1,270.8	0.0085	0.68	0.15	0.00	7.69	0.90			**1,307.6**	0.027	8.13	0.87	0.03	11.11	0.98
	Cu	**4**	**63.5**	0.0014	0.21	0.01	2.92	0.08	0.86	**Zn**	**4**	**65.3**	0.012	0.55	0.86	0.002	-1.38	0.90
			158.5	0.0008	0.83	0.86	1.55	0.10	0.93			**163.4**	0.014	0.49	0.84	0.01	0.90	0.95
			317.7	0.021	2.40	0.93	0.27	3.23	0.99			**327**	0.023	2.09	0.71	0.14	3.57	0.99
			635.4	0.0074	3.16	0.93	0.0007	6.67	0.92			**653.8**	0.024	4.57	0.95	0.02	4.55	0.91
			1,270.8	0.026	10.47	0.94	0.007	12.5	0.86			**1,307.6**	0.027	11.48	0.91	0.003	10.00	0.90
BC350	**Cu**	**6**	**63.5**	0.011	1.41	0.46	0.008	2.44	0.99	**Zn**	**6**	**65.3**	0.004	0.99	0.12	0.09	0.8	0.89
			158.5	0.018	1.48	0.55	0.16	2.56	0.98			**163.4**	0.012	1.48	0.91	0.15	1.64	0.98
			317.7	0.018	2.40	0.58	0.36	5.26	0.99			**327**	0.016	1.20	0.73	0.07	1.49	0.91
			635.4	0.017	3.47	0.49	0.48	8.33	0.99			**653.8**	0.013	2.63	0.63	0.15	4	0.99
			1,270.8	0.0039	2.40	0.03	0.06	8.33	0.99			**1,307.6**	0.026	6.17	0.87	0.05	9.09	0.99
	Cu	**5**	**63.5**	0.017	0.32	0.42	0.34	0.54	0.91	**Zn**	**5**	**65.3**	0.015	0.25	0.96	0.37	0.25	0.93
			158.5	0.018	0.83	0.65	0.12	1.18	0.89			**163.4**	0.008	1.58	0.91	0.005	2.33	0.92
			317.7	0.02	1.38	0.75	0.23	2.17	0.99			**327**	0.005	3.55	0.90	0.06	2.22	0.94
			635.4	0.01	1.62	0.25	0.87	3.23	0.99			**653.8**	0.025	5.89	0.90	0.07	8.33	0.99
			1,270.8	0.017	5.25	0.68	0.01	3.45	0.82			**1,307.6**	0.032	13.49	0.95	0.006	12.5	0.85
	Cu	**4**	**63.5**	0.01	0.50	0.95	0.01	0.78	0.87	**Zn**	**4**	**65.3**	0.01	0.20	0.77	0.01	0.47	0.90
			158.5	0.01	0.16	0.96	0.77	0.14	0.87			**163.4**	0.013	0.30	0.82	0.07	0.37	0.91
			317.7	0.01	2.57	0.83	0.11	2.78	0.98			**327**	0.033	2.82	0.98	0.09	3.13	0.98
			635.4	0.008	1.32	0.95	0.06	0.97	0.91			**653.8**	0.025	2.82	0.99	0.06	3.13	0.96
			1,270.8	0.023	7.59	0.98	0.01	8.33	0.88			**1,307.6**	0.011	0.79	0.73	0.001	12.5	0.94

1

2 Continued

AC Norit	**Cu**	**6**	**63.5**	0.032	0.52	0.65	1.93	1.69	0.99	**Zn**	**6**	**65.3**	0.012	0.45	0.08	0.23	1.15	0.95
			158.5	0.012	3.80	0.83	0.06	4.17	0.91			**163.4**	0.016	4.07	0.93	0.02	4.55	0.74
			317.7	0.014	3.24	0.77	4.00	5	0.99			**327**	0.012	2.51	0.95	0.003	4.17	0.78
			635.4	0.021	2.34	0.38	1.62	11	0.99			**653.8**	0.0073	1.95	0.11	0.07	5.88	0.94
			1,270.8	0.011	6.92	0.42	2.13	12.5	0.98			**1,307.6**	0.018	6.31	0.71	3E-05	50	0.82
	Cu	**5**	**63.5**	0.0043	0.68	0.15	0.76	0.50	0.92	**Zn**	**5**	**65.3**	0.011	0.25	0.13	0.55	0.32	0.94
			158.5	0.013	2.82	0.71	0.09	1.14	0.87			**163.4**	0.02	1.62	0.30	0.17	0.84	0.91
			317.7	0.02	2.24	0.84	1.14	2.70	0.99			**327**	0.022	2.40	0.62	0.09	2.38	0.95
			635.4	0.026	4.37	0.75	0.09	5.56	0.99			**653.8**	0.021	4.68	0.68	0.09	9.09	0.99
			1,270.8	0.026	9.55	0.94	0.005	10	0.86			**1,307.6**	0.013	16.98	0.43	0.004	16.67	0.89
	Cu	**4**	**63.5**	0.023	0.69	0.55	0.07	0.45	0.76	**Zn**	**4**	**65.3**	0.015	0.32	0.13	0.22	0.23	0.74
			158.5	0.0042	0.39	0.09	0.47	0.13	0.76			**163.4**	0.012	0.33	0.21	0.13	0.56	0.72
			317.7	0.023	6.61	0.85	0.02	5.88	0.85			**327**	0.021	5.50	0.90	0.02	5.26	0.88
			635.4	0.015	3.24	0.63	0.01	2.63	0.60			**653.8**	0.028	6.61	0.69	0.008	4.35	0.83
			1,270.8	0.0079	5.89	0.26	0.49	7.14	0.94			**1,307.6**	0.0093	9.33	0.23	2.45	14.29	0.96
AC Fluval	**Cu**	**6**	**63.5**	0.02	1.26	0.80	2.01	1.35	0.99	**Zn**	**6**	**65.3**	0.0035	0.11	0.006	11.9	0.75	0.99
			158.5	0.0089	2.29	0.67	1.69	2.56	0.97			**163.4**	0.002	1.51	0.18	0.08	0.53	0.83
			317.7	0.021	3.16	0.85	0.40	4.76	0.99			**327**	0.021	2.19	0.84	0.0005	7.69	0.87
			635.4	0.025	5.37	0.82	0.25	10	0.99			**653.8**	0.017	4.37	0.93	0.11	5.56	0.98
			1,270.8	0.023	5.37	0.68	0.64	12.5	0.99			**1,307.6**	0.021	5.37	0.66	0.07	11.11	0.99
	Cu	**5**	**63.5**	0.0078	0.71	0.37	8.25	0.50	0.95	**Zn**	**5**	**65.3**	0.013	0.47	0.22	0.30	0.23	0.87
			158.5	0.011	1.66	0.93	0.17	1.45	0.91			**163.4**	0.014	1.45	0.82	0.02	1.47	0.89
			317.7	0.011	1.29	0.36	0.81	2.78	0.99			**327**	0.014	1.86	0.66	0.11	2.33	0.97
			635.4	0.038	5.37	0.92	0.08	4.55	0.98			**653.8**	0.03	8.51	0.99	0.03	10	0.97
			1,270.8	0.035	8.91	0.88	0.02	3.57	0.87			**1,307.6**	0.021	5.25	0.95	0.10	7.14	0.99
	Cu	**4**	**63.5**	0.01	0.11	0.60	6.21	0.02	0.82	**Zn**	**4**	**65.3**	0.005	0.24	0.04	1.49	0.11	0.68
			158.5	0.0097	0.32	0.20	1.46	0.10	0.91			**163.4**	0.005	0.59	0.24	1.23	0.29	0.81
			317.7	0.021	1.82	0.44	0.15	3.33	0.99			**327**	0.028	3.55	0.70	0.06	3.57	0.96
			635.4	0.015	1.23	0.47	0.10	1.19	0.84			**653.8**	0.023	3.89	0.76	0.002	6.67	0.77
			1,270.8	0.013	3.16	0.53	0.17	6.67	0.98			**1,307.6**	0.02	3.24	0.40	0.16	14.29	0.99
Biomass	**Cu**	**6**	**63.5**	0.0063	0.84	0.48	1.15	0.77	0.87	**Zn**	**6**	**65.3**	0.0062	0.15	0.50	4.66	0.11	0.96
			158.5	0.018	1.95	0.70	0.11	0.8	0.92			**163.4**	0.012	0.81	0.39	13.2	0.92	0.96
			317.7	0.017	2.57	0.96	0.05	1.30	0.85			**327**	0.0066	0.85	0.22	0.19	1.06	0.83
			635.4	0.016	3.09	0.83	0.004	2.56	0.86			**653.8**	0.016	1.86	0.65	0.02	1.92	0.64
			1,270.8	0.023	4.57	0.98	0.08	3.13	0.98			**1,307.6**	0.014	2.00	0.41	0.05	4.35	0.95
	Cu	**5**	**63.5**	0.016	0.50	0.53	1.24	0.60	0.99	**Zn**	**5**	**65.3**	0.012	0.49	0.21	0.49	0.69	0.95
			158.5	0.018	1.35	0.62	0.25	1.25	0.95			**163.4**	0.018	0.90	0.37	0.26	1.01	0.94
			317.7	0.027	2.75	0.88	0.07	2.04	0.90			**327**	0.0005	0.32	0.40	0.60	1.35	0.99
			635.4	0.01	1.58	0.22	0.07	3.70	0.97			**653.8**	0.015	2.34	0.51	0.06	3.57	0.95
			1,270.8	0.023	3.24	0.95	0.11	3.23	0.98			**1,307.6**	0.025	4.68	0.74	0.008	5.88	0.76
	Cu	**4**	**63.5**	0.013	1.00	0.66	0.36	0.50	0.93	**Zn**	**4**	**65.3**	0.0022	0.22	0.31	1.24	0.26	0.91
			158.5	0.02	0.81	0.36	0.31	1.89	0.95			**163.4**	0.0004	0.18	0.20	0.39	0.49	0.90
			317.7	0.017	1.22	0.49	0.10	2.33	0.92			**327**	0.0027	0.26	0.01	0.41	0.93	0.95
			635.4	0.0078	1.01	0.07	0.04	4.35	0.80			**653.8**	0.0058	0.46	0.05	0.28	1.27	0.99
			1,270.8	0.012	1.66	0.32	0.03	5.26	0.85			**1,307.6**	0.012	1.32	0.35	0.06	1.92	0.83

According to the results, the correlation coefficients obtained by the pseudo-second-order kinetic model as well as q_e were higher than those of the pseudo-first-order kinetic model ($R^2 < 0.90$), suggesting that the entire adsorption process was better described by a kinetic of a second-order. The goodness of the pseudo-second-order kinetic towards the experimental results was further confirmed by the smaller confidence intervals (with few exceptions for tests at pH 4) obtained between Qe(exp) and Qe(cal) (Table S1), suggesting that the

chemisorption process favored by covalent or valency forces, and sharing of electrons may be the rate-limiting step (Ho and Mckay, 1999).

3.2.2 Adsorption isotherms

Langmuir and Freundlich estimated model parameters for all adsorbents investigated are given in Table 4. According to the obtained correlation coefficient (R^2) for copper, Langmuir model fitted the experimental data better than Freundlich for the substrates investigated at different pH values (higher average R^2 value nearly 0.90), confirming a strong copper-biochar's surface interaction. Moreover, Freundlich parameter (1/n) for copper adsorbed at pH 5 and 6 was below one, confirming a Langmuir-type isotherm. On the other hand, as also observed by others (Sheet et al., 2014), zinc showed a better correlation coefficient, 1/n and k parameter for Freundlich isotherm, indicating that each metal possesses different mechanisms of adsorption.

Table 4. Langmuir and Freundlich Isotherms parameters for Cu and Zn adsorption onto BC600ACT, BC350ACT, BC600 and BC350 at different pHs.

Adsorbent	Model	Parameters	Cu			Zn		
			pH4	pH5	pH6	pH4	pH5	pH6
BC600ACT	Langmuir	Q_{max}	5.91	0.36	14.28	1.41	14	3.33
		K	0.002	0.006	0.004	0.006	0.0006	0.006
		R^2	0.94	0.88	0.93	0.98	0.57	0.88
BC600ACT	Freundlich	K_f	0.07	1.92	2.02	0.05	0.93	0.25
		1/n	2.20	0.65	0.62	1.81	0.57	1.19
		R^2	0.70	0.82	0.96	0.96	0.59	0.91
BC350ACT	Langmuir	Q_{max}	6.17	8.87	19.72	2.88	23.58	7.38
		K	0.002	0.006	0.004	0.003	0.0005	0.006
		R^2	0.89	0.97	0.96	0.75	0.36	0.98
BC350ACT	Freundlich	K_f	1.05	2.18	2.56	1.01	1.03	1.26
		1/n	0.56	0.43	0.65	0.30	0.75	0.72
		R^2	0.86	0.84	0.97	0.26	0.85	0.97
BC600	Langmuir	Q_{max}	7.69	7.19	14.51	2.02	22.22	11
		K	0.002	0.003	0.005	0.008	0.0005	0.002
		R^2	0.20	0.88	0.98	0.93	0.73	0.89
BC600	Freundlich	K_f	0.02	1.45	1.88	0.05	1.07	0.19
		1/n	1.91	0.43	0.77	1.91	0.76	1.48
		R^2	0.85	0.63	0.98	0.96	0.78	0.93
BC350	Langmuir	Q_{max}	0.71	2.98	13.21	1.85	5.31	9.34
		K	0.005	0.006	0.003	0.003	0.002	0.002
		R^2	0.94	0.94	0.94	0.88	0.93	0.85
BC350	Freundlich	K_f	0.08	1.16	2.08	0.03	0.73	0.44
		1/n	2.21	0.19	0.52	2.06	0.85	0.93
		R^2	0.78	0.13	0.90	0.96	0.85	0.94
AC norit	Langmuir	Q_{max}	2.85	12.34	13.36	5.34	6.75	5.15
		K	0.011	0.01	0.038	0.001	0.017	0.033
		R^2	0.97	0.99	0.96	0.94	0.86	0.98
AC norit	Freundlich	K_f	0.14	0.87	2.38	0.03	0.76	1.90
		1/n	1.326	0.70	0.57	2.05	0.92	0.39
		R^2	0.63	0.95	0.92	0.89	0.66	0.56
AC fluval	Langmuir	Q_{max}	1.66	6.06	17.54	2.64	8.29	14.7
		K	0.017	0.017	0.022	0.0006	0.01	0.009
		R^2	0.99	0.98	0.84	0.79	0.76	0.31
AC fluval	Freundlich	K_f	0.14	1.06	1.74	0.043	1.10	0.34
		1/n	1.22	0.53	0.66	1.92	0.67	1.11
		R^2	0.71	0.91	0.93	0.94	0.69	0.95

1

2

3.2.3 Effect of pyrolysis temperature

The adsorption of copper and zinc at pH 6 by raw *Miscanthus x giganteus* biomass, BC pyrolyzed at 350 and 600°C is shown in Figure 4. Experimental results showed a higher removal capacity of BC600 respect to BC350 and raw biomass. Statistical analysis revealed a significantly higher capacity of copper removal by BC600 compared to BC350, while for zinc this difference was statistically reported to be non-significant. Similar tendencies were also observed for both metals (Cu and Zn) at pH 4 and pH 5 (data not shown).

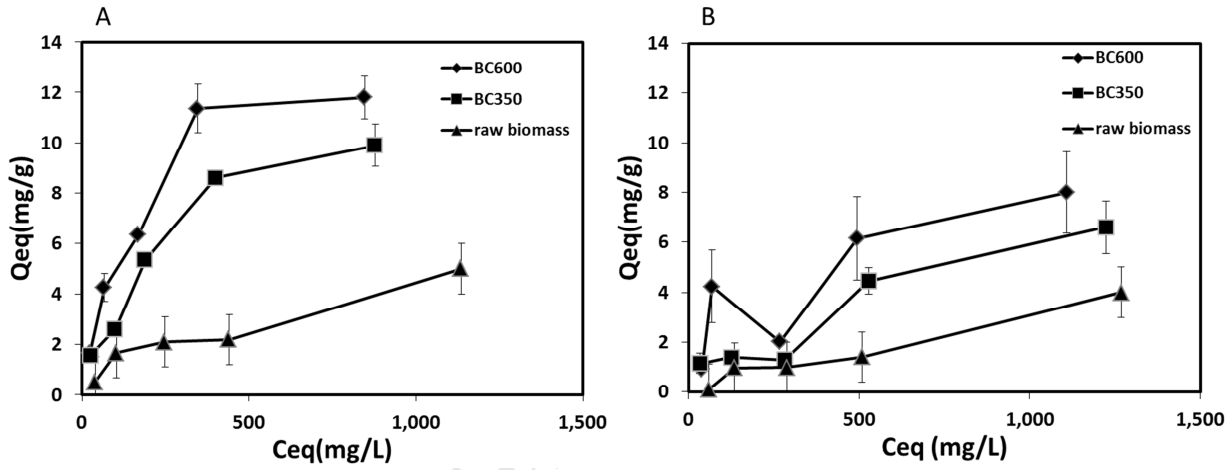

Figure 4. Uptake capacity of metals by BC600, BC350 and raw biomass for Cu (A) and Zn (B), respectively at pH6.

Figure 4 shows the impact of pyrolysis temperature on the removal capacity of biochar. This trend is in line with the results illustrated in Table 1, which showed a higher pore size of BC600 respect to BC350. As observed by others (Kim et al., (2012), during pyrolysis, the possible loss of volatile matter fosters the removal of functional groups elements (H, O and N), the atomic ratio reduces, amorphous carbon increase and microstructure develops (Table 1 and 2). These characteristics can favor adsorption processes by which van der Waals forces are involved, while for BC350 cation exchange might be favored, due to the presence of carboxyl functional groups. These results are in accordance with the elemental analysis

results (Table 1) and FT-IR results (Table 2), which showed a decrease of H, O and N elements with consequent reduction of functional groups and the shift to an aromatic structure. Moreover, the predominant aromatic structure of BC600 provides π-electron density, which is known to bond metal cation to carbon, resulting in the formation of organometallic compounds (Harvey et al., 2011). Similarly, other researchers (Kolodynska et al., 2012), showed that biochars produced at high pyrolysis temperature had higher metal adsorption capacities.

3.2.4 Effect of chemical activation by H_2O_2

The chemical modification was investigated by using hydrogen peroxide. As a matter of fact, being H_2O_2 a strong oxidizing agent ($E0_{H2O2/H2O}$ = 1.78 V) it could provide enough oxidizing power to transform hydroxyl and aldehyde groups into carboxylic ones, thereby enhancing the coordination capability and, eventually, the sorption capacity. As illustrated in Figure 5, the chemical activation by H_2O_2 showed two main results: BC600ACT did not show any enhanced adsorption capacity respect to BC600, while BC350ACT showed an enhanced removal capacity respect to BC350. Despite substantiation that the chemical activation by H_2O_2 lead to increase the oxygen-containing functional groups as indicated in Table 2 and metal-complexing functional groups (Fig. 1), particularly carboxyl groups which enhance the metal adsorption capacity (Xue et al., 2012), there are also examples that exhibit a lesser effect (Yin et al., 2007).

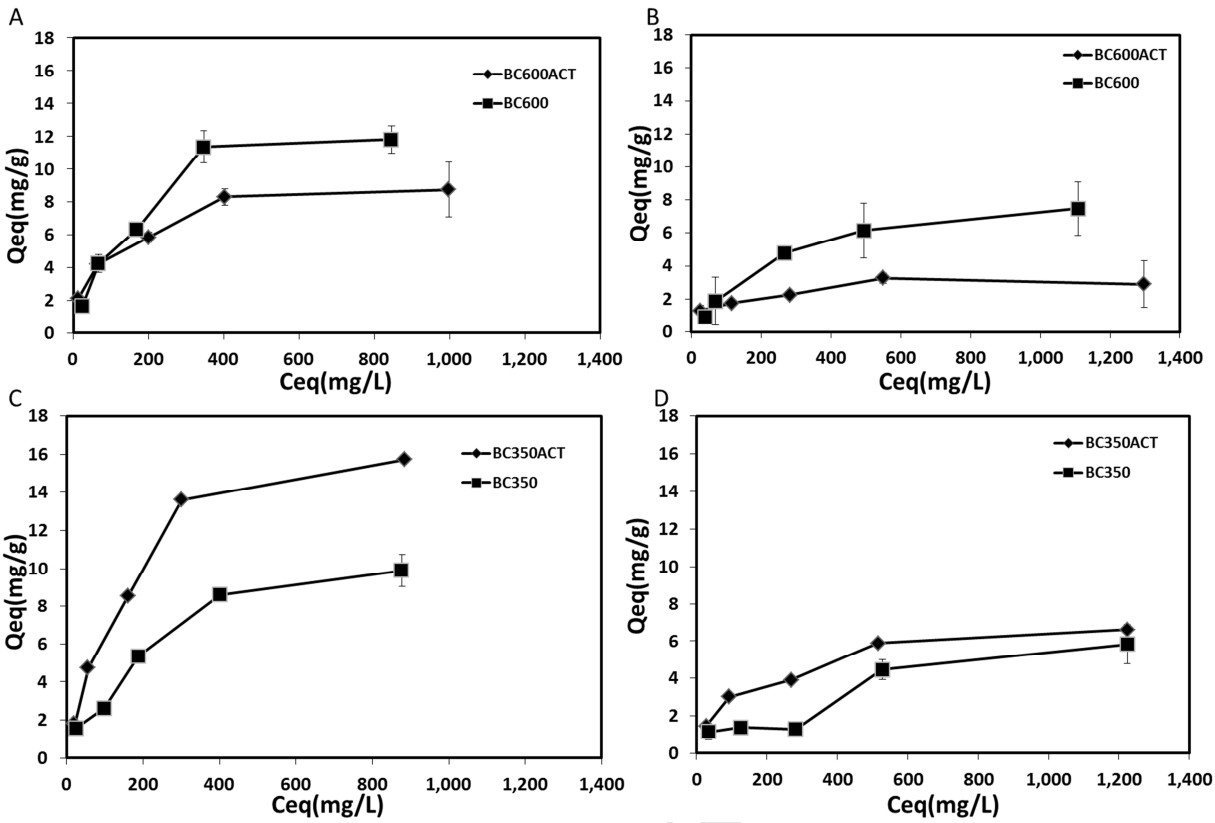

Figure 5. Effect of H_2O_2 activation on BC600 and BC350 for Copper (A-C) and zinc (B-D) at pH6.

The reduced adsorption capacity of BC600ACT respect to BC600 is given by a detrimental effect of the chemical oxidation on the physical aspect of the biochar. Indeed, along with a negligible change in BET surface area, BC600 ACT had a reduced pore size (Table 1) that may be attributable to the destruction of porous structure and textural characteristic within BC due to the severe oxidation (Yin et al., 2007). Moreover, due to an enhanced dehydration during the pyrolysis, the biochar produced at 600°C had a lower content of electron-enriched functional groups, thus resulting into a negligible chemical activation. Conversely, chemical activation improved notably the physic-chemical characteristics of biochar pyrolyzed at lower temperature, showing the highest BET surface area, highest oxygen content, highest O/C and H/C ratios (Table 1 and 2), and increased intensity of the O-H stretching of the hydroxyl groups at 3200-3400 cm^{-1} (Fig. 1), reflecting in a higher adsorption capacity. The greater effect of oxidation on biochar pyrolyzed at lower temperature could be due to the lower

degree of fused aromatic C structures (Kim et al., 2011). The correlation between effectiveness of H_2O_2 treatment and biochar pyrolysis temperature was also observed by Xue et al. (2012) and Wang et al. (2016) which, respectively reported the positive effect of H_2O_2 modification on biochar pyrolyzed at 300° C and a non-relevant effect of H_2O_2 activation on biochar pyrolyzed at 600° C in terms of cations removal capacity.

3.2.5 Effect of pH

The effect of pH on the removal efficiency is shown in Figure 6. Given the higher hydrogen ion competition at lower pH, both metals were adsorbed in larger extent at higher pH values. Indeed, at higher pH values, the weakly acidic nature of the active sites (carboxyl groups) of the biochar, favors the deprotonation process and increases the negative charge of biochar's surface, facilitating the metals cations uptake (Kolodynska et al., 2012)). Similar studies have observed an increase of metals' uptake with increasing the pH up to five, claiming as main factor the competition between protons and metal cations for surface sorption sites on the biochars (Chen et al., 2011; Liu and Zhang, 2009; Mohan et al., 2007). Moreover, the metals' uptake increased with the metals' concentration probably due to the fact that low copper and zinc concentrations were not enough to consume the alkali ions released by biochar's surface.

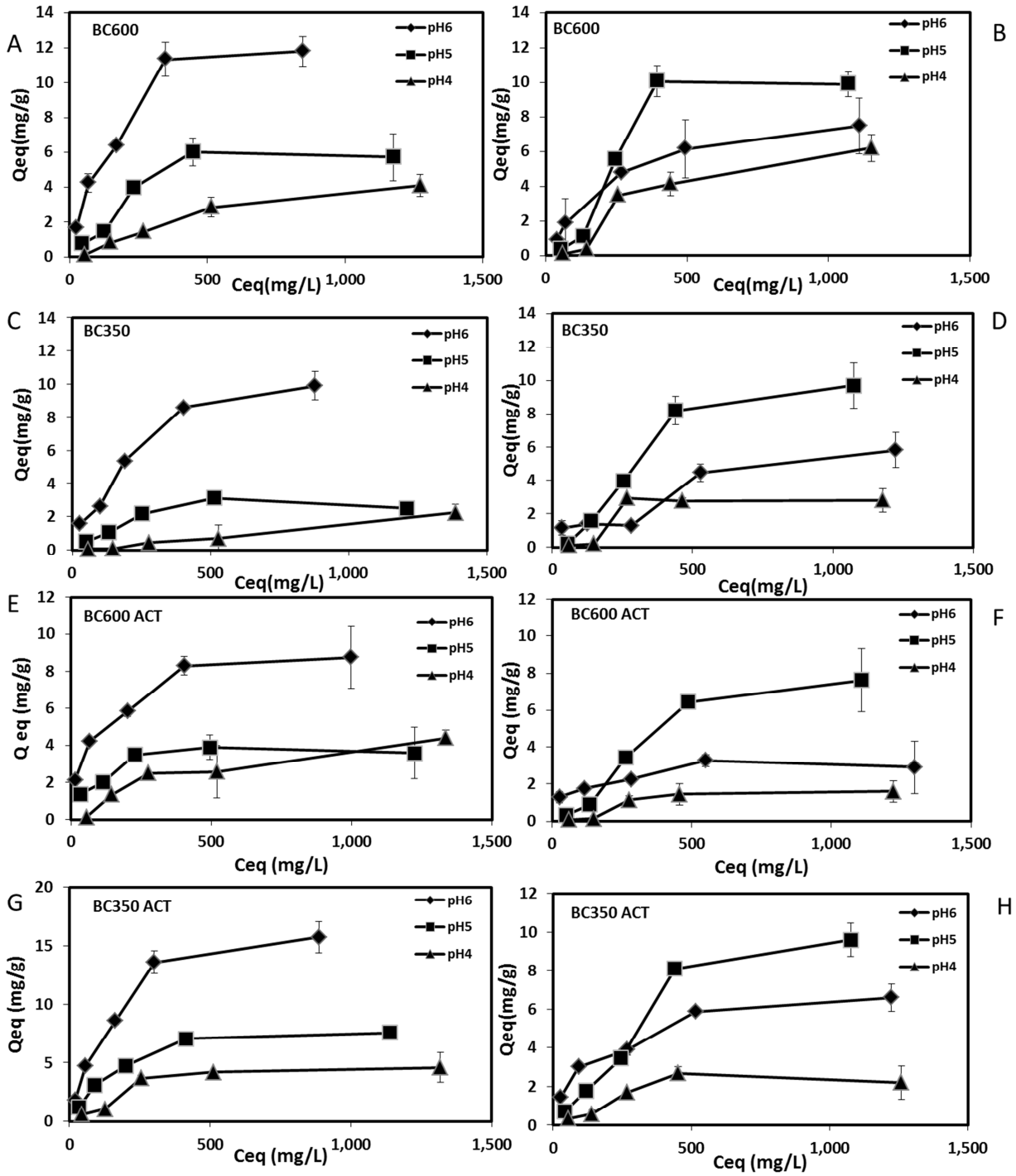

Figure 6. Effect of pH value on the adsorption capacity of Miscanthus biochar: BC600 (A and B for Cu and Zn, respectively); BC350 (C and D for Cu and Zn, respectively); BC600ACT (E and F for Cu and Zn, respectively); BC350ACT (G and H for Cu and Zn, respectively).

Under the pH range investigated in this study (4-6), maximum copper removal was at pH 6, while zinc at pH 5. As reported by Harvey et al. (2011), heavy metals are predominately adsorbed via electrostatic interactions, while other mechanisms such as ion exchange and

Cπ–metal bonding by basic carbon are less favoured. At higher pH, electrostatic interactions are favoured by active sites deprotonated, facilitating copper uptake (Mc Bride, 1994; Fontes et al., 2000). However, despite the pH was kept under control during the experiments, it cannot be excluded the formation of copper (hydr)oxide precipitation which may hinder the interaction between zinc cations and biochar's active site (Li et al., 2013). All biochars investigated showed a preferential adsorption of copper at pH 6 while zinc at pH 5 (Figure 6). Among the biochars investigated, the highest adsorption amount was obtained by BC350 ACT for copper (15.7 mg/g), however for all biochars used copper showed a stronger affinity respect to zinc, as well as demonstrated by other studies (Chen et al., 2011; Seco et al., 1997;). Importantly, biochars' adsorption capacities were comparable with AC fluval and AC norit (activated carbons) tested in parallel in this study (Table 5), and with other biochars reported in literature, such as animal manure biochar, hardwood biochars and corn-straw derived biochar (between 5 to 6 mg/g, 12.51 and 6.79 mg/g, respectively) (Kolodynska et al., 2012; Chen et al., 2011), confirming the effectiveness of *Miscanthus x giganteous* derived biochar to remove copper and zinc.

Table 5. Copper and zinc adsorption (mg/g) for biomass, BC350ACT, BC600ACT, BC350 and BC600, AC Fluval and AC Norit GAC. Results show averages ± standard error (n=2).

Adsorbent	**Cu (mg/g)**			**Zn (mg/g)**		
	pH 4	**pH 5**	**pH 6**	**pH 4**	**pH 5**	**pH 6**
BC600 ACT	4.3± 0.4	3.8± 0.6	8.7±1.6	2.6±0.5	7.6±1.6	3.2±0.3
BC350 ACT	4.6±1.2	7.9± 0.4	15.7± 1.3	3.3±0.3	9.6±0.8	6.6±0.7
BC600	4.1±0.6	6.3± 0.7	11.8± 0.8	7.3±0.7	10.4±0.8	8±1.6
BC350	3±0.4	3.1± 0.4	9.9± 0.8	2.9±0.1	9.7±1.3	5.8±1
AC Norit	6.6±2.3	6.3± 0.9	11.3± 1.6	6.6±1	17.9±2.9	5±0.6
AC Fluval	5.5±0.9	4.7±0.1	11.1± 0.7	3.2±0.6	8.8±0.2	7.2±1.1
Biomass	1.67±0.7	2.2±0.2	5±0.8	1.83±0.3	3.2±0.4	4±0.6

Given the pH-dependent metals' uptake mechanisms involved for copper and zinc removal, a study about the determination of the distribution coefficient (K_d) and the selectivity coefficient (α) was conducted. As summarized in Table 6, the α values (α_1) observed at pH 6 were at least 3 times higher than those observed at pH 4 and 5, indicating a preferential

adsorption of copper to zinc at pH 6 for all biochars investigated. Conversely, according to the α_2 values, zinc showed adsorption selectivity to copper at pH 5.

The preferential adsorption of copper to zinc could be explained by the capacity of copper to form covalent bonds, and this ability can be related to ionization potential and ionic radius (softness of a metal), as derived by Misono et al. (1967). Other researchers (Basta and Tabatabai, 1992), reported that copper was preferentially adsorbed to zinc by soil on the basis of softness parameter. McBride (1994), also explained the higher affinity and preferential retention of metals by other parameters like electronegativity and ionic radii. However, Abd-Elfaltah and Wada (1981), found that the metal retention could not be predicted only from electronegativity and ionic radii. These controversial results suggests that the metal retention affinity might involve both covalent and electrostatic bonds. Therefore, it can be concluded that the higher affinity of copper respect to zinc for surface complexation and electrostatic reactions can be explained by higher electronegativity (copper= 2.0; zinc= 1.6), larger softness value (2.89 for copper and 2.34 for zinc) and hydrolysis constant (7.3-8.0 for copper and 9.0-9.4 for zinc) (Abd-Elfaltah and Wada 1981; Basta and Tabatabai, 1992; Misono et al., 1967; Shaheen et al., 2012)).

Table 6. Competitive binding behaviors of BC600ACT, BC350ACT, BC600 and BC350 for Cu^{2+} (aq), and Zn^{2+} (aq) ions. α_1: Selectivity of copper over zinc. α_2: Selectivity of zinc over copper.

Adsorbent	pH	K_d-Cu (L/g)	K_d-Zn (L/g)	α_1	α_2
BC600ACT	4	9.21	20.35	0.45	2.20
	5	0.65	14.44	0.04	22.9
	6	41.87	25.09	1.66	0.59
	4	9.61	22.53	0.43	2.32

BC350 ACT	5	8.26	17.84	0.46	2.16
	6	50.27	21.51	2.34	0.43
	4	15.31	31.86	0.48	2.08
BC600	5	9.41	18.50	0.51	1.97
	6	55.71	35.60	1.56	0.64
	4	10.05	26.49	0.38	2.64
BC350	5	1.82	18.06	0.10	9.93
	6	44.44	15.31	2.90	0.34

4. Conclusions

This study demonstrated that *Miscanthus x giganteus* derived biochars effectively remove copper and zinc from synthetic wastewater. The temperature of pyrolysis plays an important role on the physic-chemical structure of biochar, affecting the metal removal capacity. Biochar pyrolyzed at higher temperature showed an enhanced metal removal capacity for both copper and zinc. The activation of biochar by H_2O_2 resulted to be pyrolysis-temperature sensitive, leading to enhanced metals removal capacity of the biochar pyrolyzed at lower temperature (BC350 ACT) for both copper and zinc. The effect of pH revealed that zinc was predominantly removed at pH 5 while copper at pH 6, opening new interesting scenarios about the possible selective removal and recovery of these two metals by *Miscanthus x giganteus* derived biochar. Biochars' metals removal capacities resulted to be comparable with commercially available activated carbons. Overall *Miscanthus x giganteus* derived biochar could be a valid alternative to activated carbon for an efficient removal of metal ions.

Acknowledgements

This study was supported by an International Fellowship funded by the University of Rome "La Sapienza" and by the Short Term Scientific Mission (CSCM) within the COST scientific programme on Biochar as an option for sustainable resource management. The authors would

like to acknowledge the School of Chemistry and Physics of University of KwaZulu-Natal (Westville campus) for FT-IR, BET and elemental analysis.

References

Abd-Elfaltah, A., Wada. K., 1981."Adsorption of lead, copper, zinc, cobalt and cadmium by soils that differ in cation exchange materials. Soil Sci. 32, 271– 283.

Al-Wabel, M.I., Al-Omran, A., El-Naggar, A.H., Nadeem, M., Usman, A.R.A., 2013. Pyrolysis temperature induced changes in characteristics and chemical composition of biochar produced from conocarpus wastes. Bioresour. Technol. 131, 374–379.

Akbal, F., Camci, S., 2011. Copper, chromium and nickel removal from metal plating wastewater by electrocoagulation. Desalination 269 (1–3), 214–222.

Basta, N.T., Tabatabai, M.A., 1992. Effect of cropping systems on adsorption of metals by soils. III. Competitive adsorption. Soil Sci. 153, 331-337.

Bradl, H. B., 2004. Adsorption of heavy metal ions on soils and soils constituents. J. Colloid Interface Sci. 277, 1–18.

Brosse, N., Dufour, A., Meng, X., Sun, Q., Ragauskas, A., 2012. Miscanthus: a fast-growing crop for biofuels and chemicals production. Biofuel Bioprod. Bior. 6(5), 580-98.

Brunauer, S., Emmett, P.H., Teller, E., 1938. Adsorption of Gases in Multimolecular Layers. J. Am. Chem. Soc. 60 (2), 309–319.

Boudrahem, F., Soualah, A., Aissani-Benissad, F., 2011. Pb(II) and Cd(II) removal from aqueous solutions using activated carbon developed from coffee residue activated with phosphoric acid and zinc chloride. J. Chem. Eng. Data. 56 (5), 1946–1955.

Bouwman, R., Freriks, I.L.C., 1980. Low-temperature oxidation of a bituminous coal. Infrared spectroscopic study of samples from a coal pile. Fuel. 59 (5), 315-322.

Cao, X., Harris, W., 2010. Properties of dairy-manure-derived biochar pertinent to its potential use in remediation. Bioresour. Technol. 101, 5222–5228.

Chen, X.C., Chen, G.C., Chen, L.G., Chen, Y.X., Lehmann, J., McBride, M..B, Hay, A.G., 2011. Adsorption of copper and zinc by biochars produced from pyrolysis of hardwood and corn straw in aqueous solution. Bioresour Technol. 102, 8877–8884.

Cheng, C.H., Lehmann, J., Engelhard, M.H., 2008. Natural oxidation of black carbon in soils: Changes in molecular form and surface charge along a climosequence. Geochimica et Cosmochimica Acta. 72, 1598–1610.

Clifton-Brown, J.C., Breuer, J., Jones, M.B., 2007. Carbon mitigation by the energy crop, Miscanthus. Glob Change Biol. 13(11), 2296-307.

Dabrowski, A., Hubicki, Z., Podkoscielny, P., Robens, E., 2004. Selective removal of the heavy metal ions from waters and industrial wastewaters by ion-exchange method. Chemospere. 56, 91-106.

EPA, 2016. Secondary Drinking Water Standards: Guidance for Nuisance Chemicals. https://www.epa.gov/dwstandardsregulations/secondary-drinking-water-standards-guidance-nuisance-chemicals

Fontes, M.P.F. Matos, A.T., Costa, L.M., Neves, J.C.L., 2000. Competitive adsorption of zinc, cadmium, copper and lead in three highly-weathered Brazilian soils. Commun. Soil Sci. Plant Anal. 31, 2939-2958.

Fontes, M.P.F., Gomes, P.C., 2003. Simultaneous competitive adsorption of heavy metals by the mineral matrix of tropical soils. Appl. Geochem. 18, 795-804.

Fox, J., 2008. Applied regression models and generalized linear models (2nd ed.). Thousand Oaks, CA: SAGE.

Fu, F., Xie, L., Tang, B., Wang, Q., Jiang, S., 2012. Application of a novel strategy-Advanced Fenton-chemical precipitation to the treatment of strong stability chelated heavy metal containing wastewater. Chem. Eng. J. 189–190, 283–287.

Gerente, C., Lee, V.K.C., Le Cloirec, P., Mckay, G., 2007. Application of Chitosan for the Removal of Metals from Wastewaters by Adsorption—Mechanisms and Models Review. Critical Reviews in Environ. Sci. and Technol. 37, 41–127.

Gregorich, E.G., Carter, M.R., 1997. Soil Quality for Crop Production and Ecosystem Health. Developments in Soil Science. 25, 1-448.

Harvey, O.R., Herbert, B.E., Rhue, R.D., Kuo, L.J., 2011. Metal interactions at the biochar-water interface. Energetics and structure-sorption relationships elucidated by flow adsorption microcalorimetry. Environ. Sci. Technol. 45 (13), 5550-5556.

Heaton, E., Long, S., Voigt, T., Jones, M., Clifton-Brown, J., 2004. Miscanthus for renewable Energy generation: European union experience and projections for illinois. Mitig Adapt Strateg. Glob Change. 9(4), 433-51.

Houben, D., Sonnet, P., Cornelis, J.T., 2014. Biochar from Miscanthus: a potential silicon fertilizer. Plant Soil. 374:871–882.

Ho, Y.S., Mckay, G., 1999. The kinetics of sorption of divalent metal ion onto Sphagnum moss peat. Water Res. J.. 34(3), 735-742.

Huff, M.D., Lee, J.W., 2016. Biochar-surface oxygenation with hydrogen peroxide. J. Environ. Manage. 165, 17–21.

Kang, T., Park, Y., Yi, J., 2004. Highly Selective Adsorption of Pt^{2+} and Pd^{2+} Using Thiol-Functionalized Mesoporous Silica. Ind. Eng. Chem. Res. 43, 1478-1484.

Kim, P., Johnson, A., Edmunds, C.W., Radosevich, M., Vogt, F., Rials, T.G., Labb´e, N., 2011. Surface functionality and carbon structures in lignocellulosic-derived biochars produced by fast pyrolysis. Energy Fuels. 25, 4693–4703.

Kołodyńska, D., Wnętrzak, R., Leahy, J.J., Hayes, M.H.B., Kwapiński, W., Hubicki, Z., 2012. Kinetic and adsorptive characterization of biochar in metal ions removal. Chem Eng J. 197, 295–305.

Kim, H. K., Kim, J.-Y., Cho, T.S., Choi, J.W., 2012. Influence of pyrolysis temperature on physicochemical properties of biochar obtained from the fast pyrolysis of pitch pine (Pinus rigida). Bioresour. Technol. 118, 158–162.

Kwapinski, W., Byrne, C.M.P., Kryachko, E., Wolfram, P., Adley, C., Leahy, J.J., et al., 2010. Biochar from biomass and waste. Waste Biomass Valor. 1(2), 177-89.

Lagergren, S., 1898. About the theory of so-called adsorption of soluble substances. Kungl. Sv. Vetenskapsakad. Handlingar. 24, 1.

Li, N., Bai, R.B., Liu, C.K., 2005. Enhanced, selective adsorption of mercury ions on chitosan beads grafted with polyacrylamide via surface-initiated atom transfer radical polymerization. Langmuir. 21, 11780–11787.

Li, M., Liu, Q., Guo, L.J., Zhang, Y.P., Lou, Z.J., Wang, Y., Qian, G.R., 2013. Cu(II) removal from aqueous solution by Spartina alterniflora derived biochar. Bioresour. Technol. 141, 83–88.

Lim, A.P., Aris, A.Z., 2013. A review on economically adsorbents on heavy metals removal in water and wastewater. Environ. Sci. Biotechnol. 13, 163-181.

Lin, Y. H., Fryxell, G. E.. Wu, H., Engelhard, M., 2001. Selective Sorption of Cesium Using Self-Assembled Monolayers on Mesoporous Supports. Environ. Sci. Technol. 34, 3962-3966.

Liu, Z., and Zhang, F.S., 2009. Removal of lead from water using biochars prepared from hydrothermal liquefaction of biomass. J. Hazard. Mater. 167, 933–939.

Lewandowski, I., Clifton-Brown, J., Scurlock, J., Huisman, W., 2000. Miscanthus: European experience with a novel energy crop. Biomass Bioenergy. 19(4), 209-27.

Malamis, S., Katsou, E., Haralambous, K.J., 2011. Study of Ni(II), Cu(II), Pb(II), and Zn(II) removal using sludge and minerals followed by MF/UF. Water Air Soil Pollut. 218(1-4), 81-92.

Margui, E., Salvado, V., Queralt, I., Hidalgo M., 2004. Comparison of three-stage sequential extraction and toxicity characteristic leaching tests to evaluate metal mobility in mining wastes. Anal. Chem. Acta. 524, 151–159.

McBride, M.B., 1994. Environmental Chemistry of Soils. Oxford University Press, New York, NY, USA.

Melligan, F., Dussan, K., Auccaise, R., Novotny, E.H., Leahy, J.J., Hayes, M.H.B., 2012. Characterisation of the products from pyrolysis of residues after acid hydrolysis of Miscanthus. Bioresour. Technol. 108, 258-63.

Meng, J., Feng, X., Dai, Z., Liu, X., Wu, J., Xu, J., 2014. Adsorption characteristics of Cu(II) from aqueous solution onto biochar derived from swine manure. Environ. Sci. Pollut. Res. 21, 7035–7046.

Mimmo, T., Panzacchi, P., Baratieri, M., Davies, C.A., Tonon, G., 2014. Effect of pyrolysis temperature on miscanthus (*Miscanthus x giganteus*) biochar physical, chemical and functional properties. Biomass and bioenergy. 62, 149-157.

Misono, M., Ochiai, E., Saito, Y., Yoneda, Y., 1967. A new dual parameter scale for the strength of Lewis acids and bases with the evaluation of their softness. J. Inorg. Nucl. Chem. 29, 2685-2691.

Mohan, D., Pittman, C.U., Bricka, M., Smith, F., Yancey, B., Mohammad, J., Steele, P.H., Alexandre-Franco, M.F., Gomez-Serrano, V., Gong, H., 2007. Sorption of arsenic, cadmium, and lead by chars produced from fast pyrolysis of wood and bark during bio-oil production. J. Colloid. Interface Sci. 310, 57–73.

Moreira, C.S., Alleoni, L.R. F., 2010. Adsorption of Cd, Cu, Ni and Zn in tropical soils under competitive and non-competitive systems. Sci. Agric. (Piracicaba, Braz.). 67, 301-307.

Novak, J.M., Lima, I., Xing, B., Gaskin, J.W., Steiner, C., Das, K.C., Ahmedna, M.A., Rehrah, D., Watts, D.W., Busscher, W.J., Schomberg, H., 2009. Characterization of designer biochar produced at different temperatures and their effects on a loamy sand. Ann. Environ. Sci. 3, 195–206.

Seco, A., Marzal, P., Gabaldón, C., Ferrer, J., 1997. Adsorption of heavy metals from aqueous solutions onto activated carbon in single Cu and Ni systems and in binary Cu–Ni, Cu–Cd and Cu–Zn systems. J. Chem. Technol. Biotechnol. 68, 23– 30.

Shaheen, S.M., Derbalah, A.S., Moghanm, F.S., 2012. Removal of Heavy Metals from Aqueous Solution by Zeolite in Competitive Sorption System. International Journal of Environ. Sci. Deve. 3 (4), 362-367..

Sheet, I., Kabbani, A., Holail, H., 2014. Removal of Heavy Metals Using Nanostructured Graphite Oxide, Silica Nanoparticles and Silica/ Graphite Oxide. Composite Energy Procedia. 50, 130 – 138.

Sun, R.C., Tomkinson, J., 2001. Fractional separation and physico-chemical analysis of lignins from the blackliquor of oil palm trunk fibre pulping. Sep. Purif. Technol. 24(3), 529-539.

Tchounwou, P., Yedjou, C.G., patlolla, A.K., Sutton, D.J., 2012. Heavy metals toxicity and the environment. EXS. 101, 133-164.

Trevino-Cordero, H., Juárez-Aguilar, L.G., Mendoza-Castillo, D.I., Hernández-Montoya, V., Bonilla-Petriciolet, A., Montes-Morán, M.A., 2013. Synthesis and adsorption properties of activated carbons from biomass of Prunus domestica and Jacaranda

mimosifolia for the removal of heavy metals and dyes from water. Ind. Crops Prod. 42, 315–323.

Turan, N.G., Elevli, S., Mesci, B., 2011. Adsorption of copper and zinc ions on illite: Determination of the optimal conditions by the statistical design of experiments. Appl. Clay Sci. 52, 392–399.

Wang, S.H., Griffiths, P.R., 1985. Resolution enhancement of diffuse reflectance Ir-spectra of coals by fourier self-deconvolution: 1. C-H stretching and bending modes. Fuel. 64, 229–236.

Wang, X.J., Liang, X., Wang, Y., Wang, X., Liu, M., Yin, D.Q., Xia, S.Q., Zhao, J.F., Zhang, Y.L., 2011. Adsorption of copper (II) onto activated carbons from sewage sludge by microwave-induced phosphoric acid and zinc chloride activation. Desalination. 278, 231–237.

Wang, B., Lehmann, J., Hanley, K., Hestrin, R., Enders, A., 2016. Ammonium retention by oxidized biochars produced at different pyrolysis temperatures and residence times. RSC Adv. 6, 41907-41913.

Xue, Y., Gao, B., Yao, Y., Inyang, M., Zhang, M., Zimmerman, A. R., Ro, K.S., 2012. Hydrogen peroxide modification enhances the ability of biochar (hydrochar) produced from hydrothermal carbonization of peanut hull to remove aqueous heavy metals: Batch and column tests. Chem. Eng. J. 200–202, 673–680.

Yao, Y., Gao, B., Inyang, M., Zimmerman, A.R., Cao, X., Pullammanappallil, P., Yang, L., 2011. Removal of phosphate from aqueous solution by biochar derived from anaerobically digested sugar beet tailings. J. Hazard. Mat. 190, 501–507.

Yin, C.Y., Aroua, M. K., Wan Daud, W. M. A., 2007. Review of modifications of activated carbon for enhancing contaminant uptakes from aqueous solutions. Sep. Purif. Technol. 52, 403–415.

Yuan, J., Xu, R., Zhang, H., 2011. The forms of alkalis in the biochar produced from crop residues at different temperatures. Bioresour. Technol. 102, 3488–3497.

Table 3. Parameters of pseudo-first-order and pseudo-second-order kinetics models for copper and zinc adsorption onto BC600 ACT, BC350 ACT, BC600 and BC350.

Adsorbent	Metal	pH	Initial Conc. Cu	Pseudo-first-order model			Pseudo-second-order model			Metal	pH	Initial Conc. Zn	Pseudo-first-order model			Pseudo-second-order model		
			mg/L	K_1	Qe	R^2	K_2	Qe	R^2			mg/L	K_1	Qe	R^2	K_2	Qe	R^2
BC600 ACT	**Cu**	**6**	**63.5**	0.018	0.66	0.34	2.56	2.08	0.99	**Zn**	**6**	**65.3**	0.0073	0.79	0.15	0.95	1.15	0.97
			158.5	0.0028	1.11	0.88	0.28	4.55	0.99			**163.4**	0.021	1.51	0.94	0.22	2.08	0.99
			317.7	0.0076	3.31	0.22	0.31	4.35	0.99			**327**	0.012	0.47	0.42	0.11	1.22	0.87
			635.4	0.012	3.80	0.98	0.04	10.00	0.99			**653.8**	0.022	3.02	0.75	0.06	4.00	0.96
			1,270.8	0.0039	1.11	0.82	0.02	14.29	0.98			**1,307.6**	0.03	7.24	0.90	0.03	10.00	0.98
	Cu	**5**	**63.5**	0.009	0.51	0.25	1.25	1.22	0.99	**Zn**	**5**	**65.3**	0.001	0.15	0.003	1.56	0.31	0.95
			158.5	0.022	1.29	0.88	0.33	2.13	0.99			**163.4**	0.019	1.08	0.95	0.13	1.14	0.94
			317.7	0.025	2.69	0.91	0.13	3.70	0.99			**327**	0.023	1.55	0.95	0.15	1.85	0.98
			635.4	0.022	4.17	0.75	0.02	4.55	0.86			**653.8**	0.034	5.25	0.89	0.06	6.67	0.99
			1,270.8	0.013	2.82	0.92	0.08	3.23	0.97			**1,307.6**	0.003	4.68	0.12	0.03	5.56	0.92
	Cu	**4**	**63.5**	0.005	0.28	0.49	2.81	0.08	0.89	**Zn**	**4**	**65.3**	0.006	0.19	0.85	0.67	0.13	0.80
			158.5	1.E-05	1.26	0.0001	1.01	0.09	0.98			**163.4**	0.009	0.54	0.73	2.35	0.18	0.89
			317.7	0.022	1.82	0.78	0.12	2.78	0.98			**327**	0.014	2.45	0.92	0.21	2.63	0.98
			635.4	0.0002	1.78	0.001	0.25	0.89	0.99			**653.8**	0.0012	2.09	0.002	0.03	2.94	0.76
			1,270.8	0.0321	8.32	0.98	0.009	7.69	0.85			**1,307.6**	0.004	0.86	0.03	0.05	14.29	0.99
BC350 ACT	**Cu**	**6**	**63.5**	0.018	1.32	0.88	0.28	1.96	0.99	**Zn**	**6**	**65.3**	0.017	1.06	0.84	0.35	1.56	0.99
			158.5	0.027	2.51	0.88	1.21	4.55	0.99			**163.4**	0.021	1.74	0.83	0.28	3.13	0.99
			317.7	0.0008	1.78	0.03	0.33	7.14	0.99			**327**	0.024	5.37	0.95	0.004	7.14	0.93
			635.4	0.029	10.23	0.83	0.03	14.29	0.99			**653.8**	0.033	6.92	0.97	0.02	7.14	0.90
			1,270.8	0.031	10.23	0.74	0.03	16.67	0.99			**1,307.6**	0.0048	1.20	0.03	0.01	12.5	0.92
	Cu	**5**	**63.5**	0.006	0.66	0.19	0.89	1.23	0.99	**Zn**	**5**	**65.3**	0.0018	0.13	0.01	3.88	0.81	0.98
			158.5	0.022	1.51	0.78	0.43	3.13	0.99			**163.4**	0.021	2.34	0.97	0.05	2.17	0.90
			317.7	0.024	3.39	0.94	0.10	5	0.99			**327**	0.0015	1.32	0.14	0.10	2.38	0.97
			635.4	0.023	6.46	0.96	0.05	8.3	0.99			**653.8**	0.028	5.37	0.91	0.10	8.33	0.99
			1,270.8	0.034	12.30	0.95	0.0001	33.3	0.93			**1,307.6**	0.023	0.13	0.69	0.01	11.11	0.86
	Cu	**4**	**63.5**	0.016	0.66	0.98	0.24	0.67	0.95	**Zn**	**4**	**65.3**	0.015	0.49	0.95	0.37	0.5	0.95
			158.5	0.016	0.95	0.89	2.28	1.13	0.99			**163.4**	0.012	0.87	0.93	0.05	0.77	0.90
			317.7	0.023	2.82	0.81	0.08	3.75	0.98			**327**	0.013	2.88	0.89	0.07	3.33	0.97
			635.4	0.034	5.13	0.89	0.001	11.11	0.96			**653.8**	0.022	3.98	0.99	0.03	3.85	0.90
			1,270.8	0.028	7.94	0.91	0.03	6.96	0.93			**1,307.6**	0.018	3.16	0.96	0.02	2.86	0.79

BC600	**Cu**	**6**	**63.5**	0.017	1.04	0.71	0.50	1.71	0.99	**Zn**	**6**	**65.3**	0.015	0.99	0.98	0.17	1.03	0.96
			158.5	0.028	4.79	0.95	0.06	5.31	0.98			**163.4**	0.027	5.13	0.77	0.02	4.55	0.92
			317.7	0.024	2.82	0.71	0.25	6.46	0.99			**327**	0.022	2.34	0.99	0.05	2.38	0.92
			635.4	0.03	7.94	0.81	0.04	11.44	0.99			**653.8**	0.028	4.37	0.84	0.05	6.25	0.98
			1,270.8	0.034	11.48	0.69	0.01	12.99	0.89			**1,307.6**	0.034	8.51	0.79	0.02	9.09	0.94
	Cu	**5**	**63.5**	0.018	0.59	0.84	0.47	0.81	0.98	**Zn**	**5**	**65.3**	0.009	0.47	0.51	0.12	0.5	0.90
			158.5	0.014	0.92	0.56	0.50	1.47	0.99			**163.4**	0.02	1.38	0.98	0.07	1.37	0.88
			317.7	0.01	2.40	0.64	0.48	3.23	0.99			**327**	0.001	2.88	0.57	0.05	2.86	0.93
			635.4	0.025	4.79	0.86	0.06	6.67	0.98			**653.8**	0.027	6.46	0.78	0.06	11.11	0.99
			1,270.8	0.0085	0.68	0.15	0.00	7.69	0.90			**1,307.6**	0.027	8.13	0.87	0.03	11.11	0.98
	Cu	**4**	**63.5**	0.0014	0.21	0.01	2.92	0.08	0.86	**Zn**	**4**	**65.3**	0.012	0.55	0.86	0.002	-1.38	0.90
			158.5	0.0008	0.83	0.86	1.55	0.10	0.93			**163.4**	0.014	0.49	0.84	0.01	0.90	0.95
			317.7	0.021	2.40	0.93	0.27	3.23	0.99			**327**	0.023	2.09	0.71	0.14	3.57	0.99
			635.4	0.0074	3.16	0.93	0.0007	6.67	0.92			**653.8**	0.024	4.57	0.95	0.02	4.55	0.91
			1,270.8	0.026	10.47	0.94	0.007	12.5	0.86			**1,307.6**	0.027	11.48	0.91	0.003	10.00	0.90
BC350	**Cu**	**6**	**63.5**	0.011	1.41	0.46	0.008	2.44	0.99	**Zn**	**6**	**65.3**	0.004	0.99	0.12	0.09	0.8	0.89
			158.5	0.018	1.48	0.55	0.16	2.56	0.98			**163.4**	0.012	1.48	0.91	0.15	1.64	0.98
			317.7	0.018	2.40	0.58	0.36	5.26	0.99			**327**	0.016	1.20	0.73	0.07	1.49	0.91
			635.4	0.017	3.47	0.49	0.48	8.33	0.99			**653.8**	0.013	2.63	0.63	0.15	4	0.99
			1,270.8	0.0039	2.40	0.03	0.06	8.33	0.99			**1,307.6**	0.026	6.17	0.87	0.05	9.09	0.99
	Cu	**5**	**63.5**	0.017	0.32	0.42	0.34	0.54	0.91	**Zn**	**5**	**65.3**	0.015	0.25	0.96	0.37	0.25	0.93
			158.5	0.018	0.83	0.65	0.12	1.18	0.89			**163.4**	0.008	1.58	0.91	0.005	2.33	0.92
			317.7	0.02	1.38	0.75	0.23	2.17	0.99			**327**	0.005	3.55	0.90	0.06	2.22	0.94
			635.4	0.01	1.62	0.25	0.87	3.23	0.99			**653.8**	0.025	5.89	0.90	0.07	8.33	0.99
			1,270.8	0.017	5.25	0.68	0.01	3.45	0.82			**1,307.6**	0.032	13.49	0.95	0.006	12.5	0.85
	Cu	**4**	**63.5**	0.01	0.50	0.95	0.01	0.78	0.87	**Zn**	**4**	**65.3**	0.01	0.20	0.77	0.01	0.47	0.90
			158.5	0.01	0.16	0.96	0.77	0.14	0.87			**163.4**	0.013	0.30	0.82	0.07	0.37	0.91
			317.7	0.01	2.57	0.83	0.11	2.78	0.98			**327**	0.033	2.82	0.98	0.09	3.13	0.98
			635.4	0.008	1.32	0.95	0.06	0.97	0.91			**653.8**	0.025	2.82	0.99	0.06	3.13	0.96
			1,270.8	0.023	7.59	0.98	0.01	8.33	0.88			**1,307.6**	0.011	0.79	0.73	0.001	12.5	0.94

Table 4. Langmuir and Freundlich Isotherms parameters for Cu and Zn adsorption onto BC600ACT, BC350ACT, BC600 and BC350 at different pHs.

Adsorbent	Model	Parameters	Cu			Zn		
			pH4	pH5	pH6	pH4	pH5	pH6
BC600ACT	Langmuir	Q_{max}	5.91	0.36	14.28	1.41	14	3.33
		K	0.002	0.006	0.004	0.006	0.0006	0.006
		R^2	0.94	0.88	0.93	0.98	0.57	0.88
BC600ACT	Freundlich	K_f	0.07	1.92	2.02	0.05	0.93	0.25
		1/n	2.20	0.65	0.62	1.81	0.57	1.19
		R^2	0.70	0.82	0.96	0.96	0.59	0.91
BC350ACT	Langmuir	Q_{max}	6.17	8.87	19.72	2.88	23.58	7.38
		K	0.002	0.006	0.004	0.003	0.0005	0.006
		R^2	0.89	0.97	0.96	0.75	0.36	0.98
BC350ACT	Freundlich	K_f	1.05	2.18	2.56	1.01	1.03	1.26
		1/n	0.56	0.43	0.65	0.30	0.75	0.72
		R^2	0.86	0.84	0.97	0.26	0.85	0.97
BC600	Langmuir	Q_{max}	7.69	7.19	14.51	2.02	22.22	11
		K	0.002	0.003	0.005	0.008	0.0005	0.002
		R^2	0.20	0.88	0.98	0.93	0.73	0.89
BC600	Freundlich	K_f	0.02	1.45	1.88	0.05	1.07	0.19
		1/n	1.91	0.43	0.77	1.91	0.76	1.48
		R^2	0.85	0.63	0.98	0.96	0.78	0.93
BC350	Langmuir	Q_{max}	0.71	2.98	13.21	1.85	5.31	9.34
		K	0.005	0.006	0.003	0.003	0.002	0.002
		R^2	0.94	0.94	0.94	0.88	0.93	0.85
BC350	Freundlich	K_f	0.08	1.16	2.08	0.03	0.73	0.44
		1/n	2.21	0.19	0.52	2.06	0.85	0.93
		R^2	0.78	0.13	0.90	0.96	0.85	0.94
AC norit	Langmuir	Q_{max}	2.85	12.34	13.36	5.34	6.75	5.15
		K	0.011	0.01	0.038	0.001	0.017	0.033
		R^2	0.97	0.99	0.96	0.94	0.86	0.98
AC norit	Freundlich	K_f	0.14	0.87	2.38	0.03	0.76	1.90
		1/n	1.326	0.70	0.57	2.05	0.92	0.39
		R^2	0.63	0.95	0.92	0.89	0.66	0.56
AC fluval	Langmuir	Q_{max}	1.66	6.06	17.54	2.64	8.29	14.7
		K	0.017	0.017	0.022	0.0006	0.01	0.009
		R^2	0.99	0.98	0.84	0.79	0.76	0.31
AC fluval	Freundlich	K_f	0.14	1.06	1.74	0.043	1.10	0.34
		1/n	1.22	0.53	0.66	1.92	0.67	1.11
		R^2	0.71	0.91	0.93	0.94	0.69	0.95